

# How Population Growth Affects Linkage Disequilibrium

Alan R. Rogers\*

November 12, 2013

## Abstract

The “LD curve” relates the linkage disequilibrium (LD) between pairs of nucleotide sites to the distance that separates them along the chromosome. The shape of this curve reflects natural selection, admixture between populations, and the history of population size. The present article derives new results about the last of these effects. When a population expands in size, the LD curve grows steeper, and this effect is especially pronounced following a bottleneck in population size. When a population shrinks, the LD curve rises but remains relatively flat. As LD converges toward a new equilibrium, its time path may not be monotonic. Following an episode of growth, for example, it declines to a low value before rising toward the new equilibrium. These changes happen at different rates for different LD statistics. They are especially slow for estimates of  $\sigma_d^2$ , which therefore allow inferences about ancient population history. For the European human population, these results suggest a history of population growth. For several populations of human foragers, they suggest a history of population decline.

## INTRODUCTION

Linkage disequilibrium (LD) refers to the statistical association between pairs genetic loci. It is used routinely in lo-

calizing disease genes, in detecting natural selection, and in studying population history. In all of these contexts, it is necessary to account for the changes in LD caused by changes in population size.

These changes occur because inhabitants of small populations tend to be

---

\*Dept. of Anthropology, 270 S 1400 E, University of Utah, Salt Lake City, Utah 84112

close relatives. The genealogical paths that separate them are short, and this reduces the opportunity for recombination. For this reason, LD rises after a fall in population size and falls after a rise.

These effects are understood in a general way and are often studied by computer simulation (KRUGLYAK, 1999; PRITCHARD and PRZEWORSKI, 2001). Although this approach has led to important insights, our understanding is still rudimentary. The present paper will use a deterministic algorithm to explore the effects of growth, of decline, and of temporary reductions (bottlenecks) in population size. It will show that each type of history leaves a distinctive signature in the “LD curve,” which relates the LD between pairs of sites to the distance that separates them along the chromosome.

The paper uses  $\sigma_d^2$  (defined below) as a measure of LD. This choice is unusual, because  $\sigma_d^2$  has always been of secondary importance. As we shall see, however,  $\sigma_d^2$  has dynamical properties that give it deeper time depth than alternative measures of LD. It is readily estimated from data and can be predicted by a deterministic theory, which makes it easy to study the response to changes in population size. This paper will show that  $\sigma_d^2$  is of more than secondary importance. It is useful in its own right as a measure of LD.

## MATERIAL AND METHODS

### Measuring LD

Consider a pair of loci (nucleotide sites),  $A$  and  $B$ . At locus  $A$ , alleles  $A_1$  and  $A_0$  have frequencies  $a$  and  $1 - a$ . At locus  $B$ , alleles  $B_1$  and  $B_0$  have frequencies  $b$  and  $1 - b$ . The disequilibrium coefficient,  $D$ , is defined such that  $ab + D$  is the frequency of gamete type  $A_1B_1$ . The sign of  $D$  is arbitrary, depending on how one labels the alleles, so the magnitude of LD is often measured by  $D^2$ .

These measures are strongly affected by heterozygosity at the two loci, so many authors prefer the squared correlation coefficient (HILL and ROBERTSON, 1968),

$$r^2 = \frac{D^2}{a(1-a)b(1-b)}. \quad (1)$$

Unfortunately, there is no consensus regarding the expected value of this statistic, even in the simplest case of neutral loci in a randomly-mating population of constant size (compare SVED, 2009 with SONG and SONG, 2007 and DURRETT, 2008, p. 98).

OHTA and KIMURA (1969, p. 233) proposed a related measure of LD, the “squared standard linkage deviation,” which was also motivated by a desire to minimize the effect of heterozygosity.

$$\sigma_d^2 = \frac{E[D^2]}{E[a(1-a)b(1-b)]} \quad (2)$$

This measure is usually viewed as an approximation to  $E[r^2]$ . It is most useful in this role when the population size is large and constant, and both loci have appreciable heterozygosity (HUDSON, 1985). In other situations, the two parameters can differ greatly. But even when  $\sigma_d^2$  fails as an approximation, it is still useful as a measure of LD.

This is not to say that  $\sigma_d^2$  provides a complete description of variation at a pair of loci. That is a problem with multiple dimensions, which cannot be solved by any scalar-valued measure of LD (WEIR, 1996, pp. 125–127). Such measures are simplifications and are necessarily incomplete (SCHAPER *et al.*, 2012). Yet as we shall see,  $\sigma_d^2$  captures enough to provide an interesting window into the history of population size.

### Estimation of $\sigma_d^2$

One can estimate  $\sigma_d^2$  from data by replacing the expected values in Eqn. 2 with averages across the genome. For this purpose, I treat each polymorphic site (SNP) as “focal,” and compare the focal SNP with each other SNP within some given range—often 0.3 cM. From each comparison, I calculate  $D^2$  and  $a(1 - a)b(1 - b)$ . These values are tabulated separately within bins based on the distance in cM between the SNPs. After all comparisons have been tabulated,  $\hat{\sigma}_d^2$  is calculated as the sum of  $D^2$  within a bin divided by the correspond-

ing sum of  $a(1 - a)b(1 - b)$ .

To estimate uncertainties, I use a moving blocks bootstrap (LIEU and SINGH, 1992), with 300 SNPs per block. With diploid data, some genotypes may be unphased. In such cases, I use the EM algorithm to estimate  $D^2$ , as explained in the appendix.

### Deterministic evolution of $\sigma_d^2$

Under neutral evolution with constant population size,  $\sigma_d^2$  converges to an equilibrium value (MCVEAN, 2002; OHTA and KIMURA, 1971). In addition, several authors have introduced recurrence equations, which make it possible to study the transient behavior of  $\sigma_d^2$  after changes in population size (HILL, 1975; STROBECK and MORGAN, 1978; WEIR and COCKERHAM, 1974). The model of STROBECK and MORGAN (1978) allows faster calculations but is less numerically stable than that of HILL (1975). I present some results using the former model of but focus primarily on the latter. In the appendix, I summarize Hill’s model and show that it holds not only under the mutational model that he studied, but also under the model of infinite sites (KIMURA, 1969). It is thus appropriate for use with DNA sequence data.

For bootstrap confidence intervals, I accelerate these calculations by using Eqn. 6 of the appendix to approximate a system of ordinary differential equa-

tions, which is then solved using standard software.

## Simulations

The various methods were evaluated against simulated data generated by MACS (CHEN *et al.*, 2009). Simulation results in Fig. 1 are based on my own coalescent program, written in C.

## Sampling bias

Drawing a sample is equivalent to one generation of evolution with a very small population—one whose size equals the sample size. Because drift introduces LD, there is much more LD in a sample than in the population from which it was drawn.

HUDSON (1985, Eqn. 6) showed that sampling bias in  $r^2$  equals  $1/n$ , when the sample consists of  $n$  gametes. To correct sampling bias in  $\hat{\sigma}_d^2$ , I use the model of HILL (1975) or STROBECK and MORGAN (1978) to project the state vector forward one generation, with the population size set equal to the sample size.

## RESULTS

### $\hat{\sigma}_d^2$ is average $r^2$ , weighted by heterozygosities

Eqn. 2 is equivalent to

$$\sigma_d^2 = \frac{E[H_A H_B r^2]}{E[H_A H_B]}, \quad (3)$$

where  $H_A = 2a(1 - a)$  is the heterozygosity at locus  $A$  and  $H_B$  is that at locus  $B$ . This implies that  $\sigma_d^2$  is the expectation of  $r^2$  weighted by the product of the two heterozygosities.

This weighting also carries over to the estimate,  $\hat{\sigma}_d^2$ , which is obtained by replacing expectations with averages. Such estimates will be insensitive to loci with low heterozygosity and, for this reason, also insensitive to sequencing error. They should be useful with low-coverage sequence data.

### Loci with high heterozygosity have deep gene trees.

Weighting by heterozygosity is also of interest because it exaggerates the influence of unusually deep gene trees. At some given nucleotide position, let  $T$  represent the age of the last common ancestor of the sample. I will call this the “depth” of the gene tree for that nucleotide position. GRIFFITHS and TAVARÉ (1998, Eqn. 1.5, p. 276) derive the conditionally expected depth,  $E[T|x, n]$ , given that  $x$  copies of the derived allele were observed in a sample of haploid size  $n$ . Given the heterozygosity, we can solve for  $x$ , but we cannot tell the derived from the ancestral allele. It may be present in  $x$  copies or in  $n - x$ . At mutation-drift equilibrium, however, these alternatives have probabilities proportional to  $1/x$  and  $1/(n - x)$  (FU, 1995, Eqn. 1). Us-

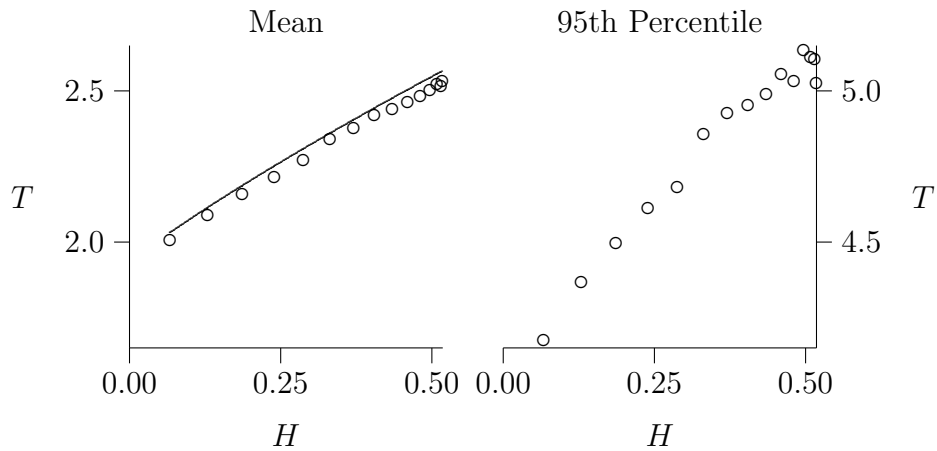


**Figure 1: The depth,  $T$ , of gene genealogy given heterozygosity,  $H$ .** The left and right panels show the mean and the 95th percentile. Solid line shows expected values, based on the model of GRIFFITHS and TAVARÉ (1998, Eqn. 1.5, p. 276). Open circles show results from coalescent simulations. These results assume a sample of 30 individuals and a mutation rate of 0.02 per  $2N$  generations. The slope is greater in the right panel than the left, indicating that heterozygosity has a stronger effect on the upper tail of the distribution than on the mean.

ing these values as weights, I average  $E[T|x, n]$  and  $E[T|n - x, n]$  in order to calculate expected tree depth given heterozygosity. The results are shown as a solid line in Fig. 1. As the figure shows, tree depth increases with heterozygosity. Simulated values—shown as open circles—agree closely with the theory.

Simulated values also allow us to examine the upper tail of the distribution, as seen in the right panel of Fig. 1. The 95th percentile of tree depth increases with heterozygosity even more steeply than does the mean. Thus, heterozygosity has an exaggerated effect on the upper tail of the distribution.

Geneticists often study loci selected for their high heterozygosity (CLARK *et al.*, 2005; LEWONTIN, 1967; ROGERS and JORDE, 1996). A sample of loci selected in this fashion will have gene trees that are unusually deep, especially in the upper tail of the distribution.

Because  $\sigma_d^2$  is weighted by heterozygosity, it exaggerates the influence of these deep gene trees. For this reason, it should be sensitive to earlier portions of a population’s history. Following a change in population size, it should converge more slowly to the new equilibrium.

### Effect of population growth

LD will decline following an expansion of population size, because genetic drift is weaker in large populations and pro-

duces less LD. This process is illustrated in Fig. 2, which shows the effect of an expansion from size  $2N = 10^3$  to  $2N = 10^5$ . The LD curve of the initial population (labeled  $t = 0$ ), represents an equilibrium between mutation, drift, and recombination. After the expansion, the LD curve will eventually converge to a new equilibrium, which is labeled  $t = \infty$ . This new equilibrium, however, is reached only gradually.

LD is measured by  $\sigma_d^2$  in the left panel and by  $r^2$  in the right. The dashed lines were calculated using the method of HILL (1975), and the open circles were estimated from data simulated using MACS (CHEN *et al.*, 2009). Note that  $\sigma_d^2$  is still far from equilibrium at generation 500 and does not approach equilibrium until about generation 1500.

The situation is very different in the right panel, where LD is measured using  $r^2$ . By generation 500,  $r^2$  is close to equilibrium. At the left edge of the graph, it is slightly *below* the equilibrium. We’ll return to this point later, but for the moment, note simply that  $r^2$  converges much faster than  $\sigma_d^2$ . For this reason, the two measures are useful for studying different time scales. We learn from  $r^2$  about the recent past and from  $\sigma_d^2$  about more ancient events. Presumably, this difference arises because  $\sigma_d^2$  is weighted toward loci with high heterozygosity. As shown in Fig. 1, this weighting makes it more sensitive to the distant past.

Returning to the left panel of Fig. 2,

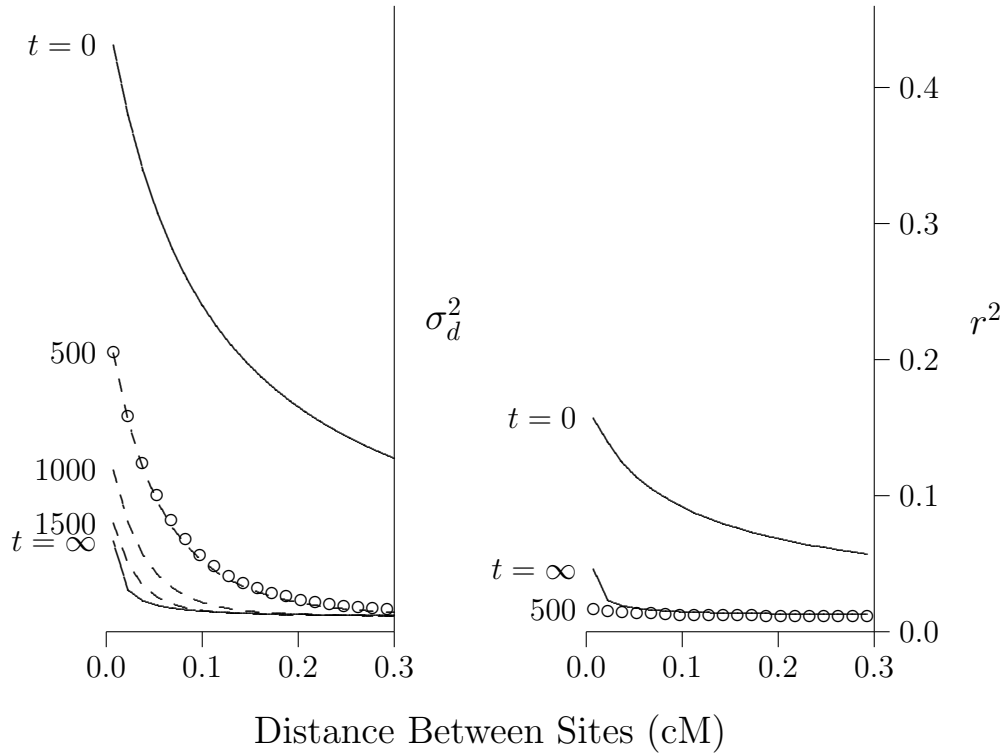


**Figure 2: Effect of population expansion on the LD curve.** The population grew suddenly at time  $t = 0$  from  $2N = 10^3$  to  $10^5$ . *Left panel:* LD is measured by  $\sigma_d^2$ . Solid lines show the predicted values at the initial equilibrium ( $t = 0$ ) and at the eventual equilibrium ( $t = \infty$ ). Dashed lines show a series of transient states that occur at various values of  $t$ , the number of generations since the expansion. These lines are all calculated using the method of HILL (1975). Open circles show values simulated using MACS (CHEN *et al.*, 2009) for  $t = 500$ . *Right panel:* LD is measured by  $r^2$ , and points and lines are based on computer simulation. The mutation rate is  $u = 10^{-8}$  per site per generation, and the haploid sample size is 100.

note that the right portion of the curve converges faster than the left. This is because the post-expansion population is large, and genetic drift is weak. The dynamics are therefore dominated by recombination, which is stronger on the right side of the graph. The result is that midway through the process—say at generation 500—the LD curve declines very steeply. Thus, a steeply declining LD curve is the signature of recent population growth. Steeply declining LD curves can also be produced by gene conversion (FRISSE *et al.*, 2001). The two effects should be separable, however, because population growth affects LD over a much wider range of recombination rates. The effect of population growth on the LD curve was first described by KRUGLYAK (1999).

### The method of HAYES *et al.*

Figure 2 suggests that  $\sigma_d^2$  is likely to be of greater use than  $r^2$  in inferring the ancient history of population size. Yet the latter statistic is often used instead (HAYES *et al.*, 2003; MCEVOY *et al.*, 2011; TENESA *et al.*, 2007), using a method that is based on the formula  $E[r^2] \approx \rho$ , where

$$\rho = 1/(1 + 4Nc) \quad (4)$$

Here,  $N$  is population size, and  $c$  is the recombination rate (SVED, 1971; SVED and FELDMAN, 1973). Although this formula has been criticized (LITTLER,

1973, p. 272; MCV EAN, 2002, pp. 987–988; DURRETT, 2008, p. 98), it is still used as a basis for inference.

HAYES *et al.* (2003) study a generalization of  $r^2$  and argue from simulations that the expectation of this statistic is approximately equal to  $\rho$ . Furthermore, this approximation even works for populations that have increased in size at a constant linear rate, provided that one interprets  $N$  as the population size that obtained  $1/2c$  generations in the past. By inverting Eqn. 4, they are able to estimate  $N$  over a wide range of values in  $c$ , which correspond under their model to different points in the past. TENESA *et al.* (2007) work directly with  $r^2$ , but estimate the history of population size in the same way. This method is also used by MCEVOY *et al.* (2011).

Of course, no population can increase linearly forever, so the period of linear increase must end at some point in the past. Furthermore, the method has also been used to infer more complex patterns of growth, including bottlenecks (HAYES *et al.*, 2003; MCEVOY *et al.*, 2011; TENESA *et al.*, 2007). Thus, it is worth evaluating the method in a broader context.

Figure 3 considers a population that expands suddenly in size and is observed 500 generations later. In both panels, the solid lines show predicted LD. In the left panel, LD is measured by  $\hat{\sigma}_d^2$  and predicted by  $\sigma_d^2$  (HILL, 1975). In the right panel, it is measured by  $r^2$  and

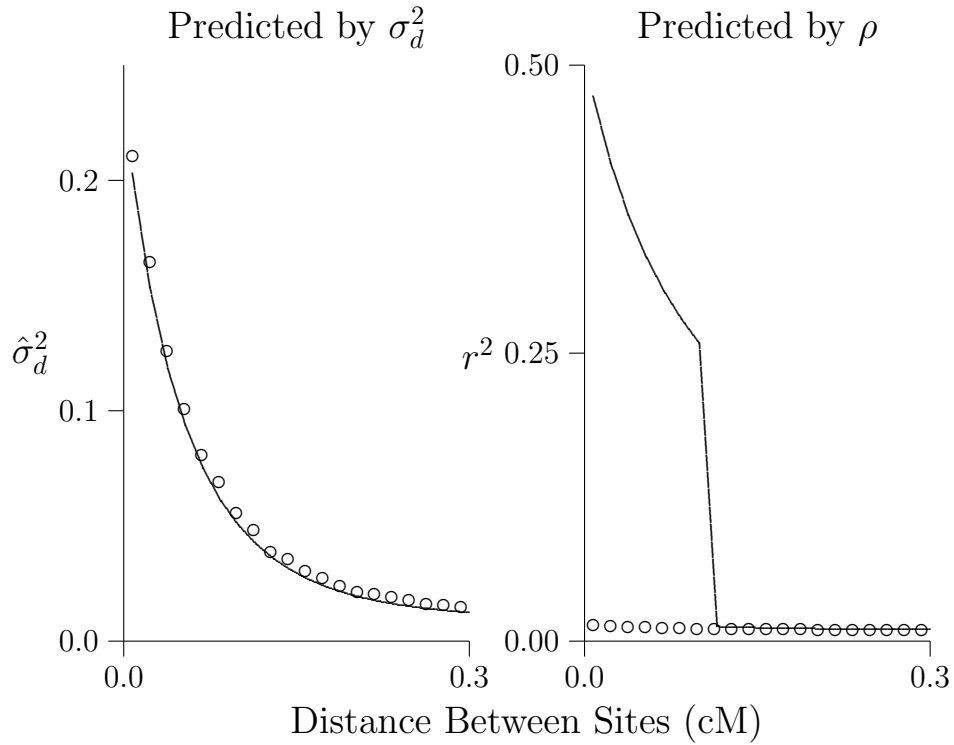


**Figure 3: Predicted and simulated LD.** Each panel shows the same population 500 generations after expansion from  $2N = 10^3$  to  $10^5$ . Lines show values predicted by  $\sigma_d^2$  (left panel, (HILL, 1975)) and by  $\rho$  (right panel, (HAYES *et al.*, 2003)). Open circles show results estimated from simulations.

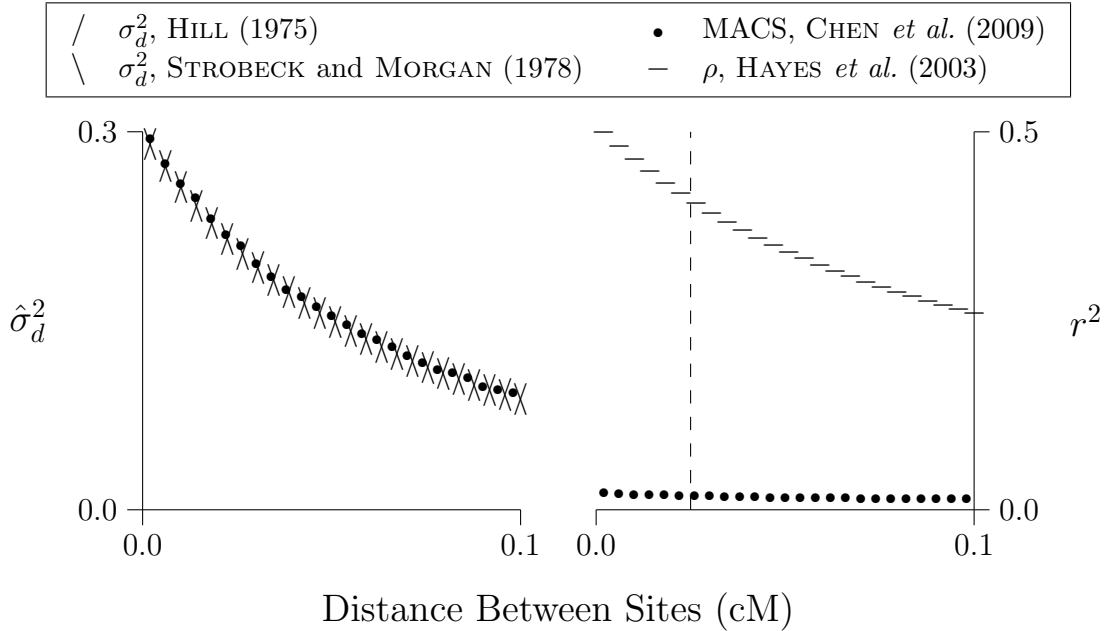


**Figure 4: Linkage disequilibrium ( $\hat{\sigma}_d^2$  or  $r^2$ ) after an episode of linear growth.** The population begins at mutation-drift equilibrium with  $2N = 10^3$  and then grows linearly to  $2N = 10^6$  over a period of 300 generations. Linear growth is approximated by 20 epochs of 15 generations, within each of which  $2N$  is constant. In the right panel, the region to the right of the vertical line corresponds to the period of linear growth, according to the model (HAYES *et al.*, 2003). All calculations assume that  $u = 1.48 \times 10^{-8}$  and  $c = 10^{-8}$  per nucleotide. Simulations involve  $10^9$  base pairs of DNA, which are sequenced in a sample of 100 homologous chromosomes.

predicted by  $\rho$  (HAYES *et al.*, 2003). The open circles show values simulated using MACS (CHEN *et al.*, 2009). In the context of this population history,  $\sigma_d^2$  provides excellent predictions but  $\rho$  does not.

Figure 4 evaluates  $\rho$  against a history involving 300 generations of linear population growth, approximated as a series of 20 steps. Linear growth is the context in which the model was originally validated, so it ought to work well here. Yet this is not the case. The period of linear growth corresponds to the region to the right of the dashed line in the right panel of Fig. 4. At least in this region, predicted and simulated values should match. Yet as before,  $\sigma_d^2$  predicts well,  $\rho$  poorly.

Finally, Fig. 5 evaluates  $\rho$  and  $\sigma_d^2$  against a history of constant population size. In this case,  $\rho$  is a fair approximation to  $\hat{\sigma}_d^2$  but does not provide a useful approximation of  $r^2$ . On the other hand,  $\sigma_d^2$  does provide an accurate prediction of  $\hat{\sigma}_d^2$ .

There may be cases in which  $\rho$  predicts  $r^2$  with accuracy, but this is not so in any of the cases studied here. It seems unlikely that  $\rho$  will be useful as a basis for inference in real populations.

### Effect of population collapse

A collapse in population size produces an effect on the LD curve very different from that of population growth. This is

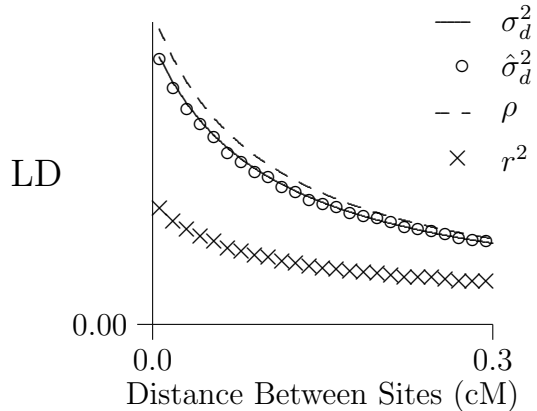


**Figure 5: LD curve under constant population size.** Simulated values of  $r^2$  and  $\hat{\sigma}_d^2$  were generated using MACS (CHEN *et al.*, 2009).  $\sigma_d^2$  was calculated using the method of HILL (1975), and  $\rho$  was calculated from Eqn. 4. All calculations assume a population size of  $2N = 10^3$  and a sample of 60 chromosomes.

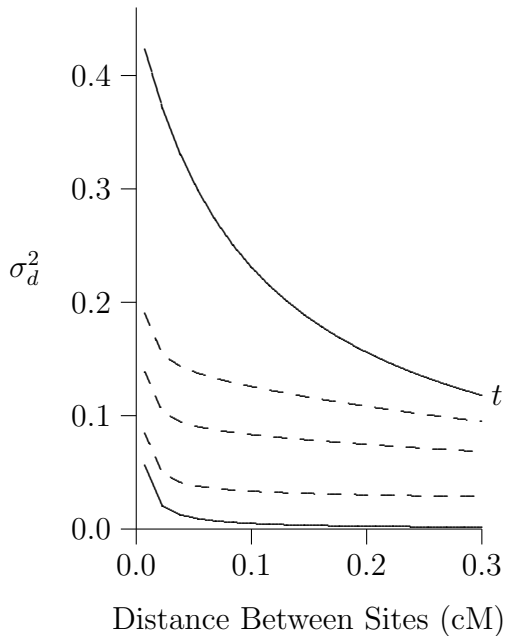


**Figure 6: Effect of population collapse on the LD curve.** At time  $t = 0$ , this population collapsed in size from  $2N = 10^5$  to  $10^3$ . Other details are as in Fig. 2.

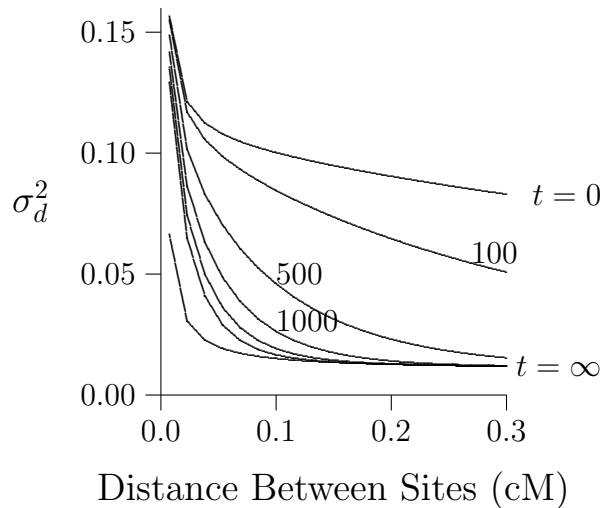


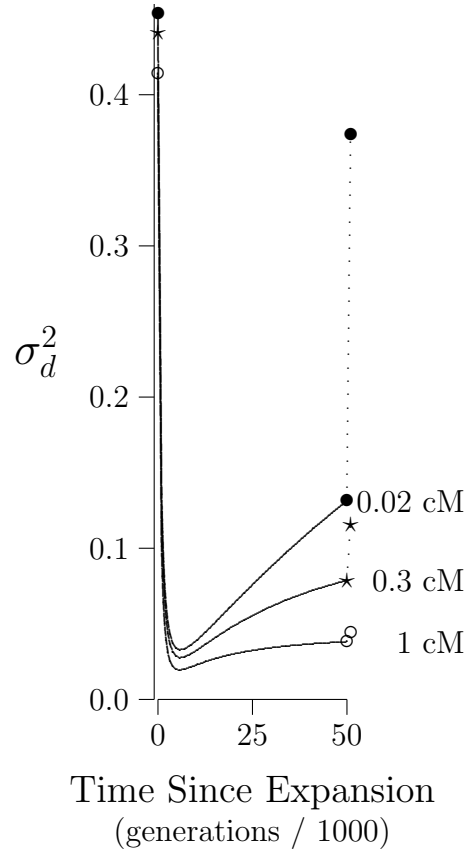
**Figure 7: Effect of a 100-generation bottleneck in population size.** The curves show  $\sigma_d^2$  at various points after recovery from a 100-generation bottleneck, during which the population had size  $2N = 10^3$ . Before and after the bottleneck, its size was  $10^5$ . Other details as in Fig. 2.

shown in Fig. 6, which illustrates two important points. First, the whole process is over very quickly. Even with  $\sigma_d^2$ , we cannot look very far into the past. Second, the transient curves (the dashed lines) are quite flat. As time passes, the initial curve (at  $t = 0$ ) is elevated without much change in shape. Presumably, this is because the effect of drift is dominant in a small population, so that differences in recombination rate do not matter much. The result is that the LD curve becomes high but flat after a collapse in population size.

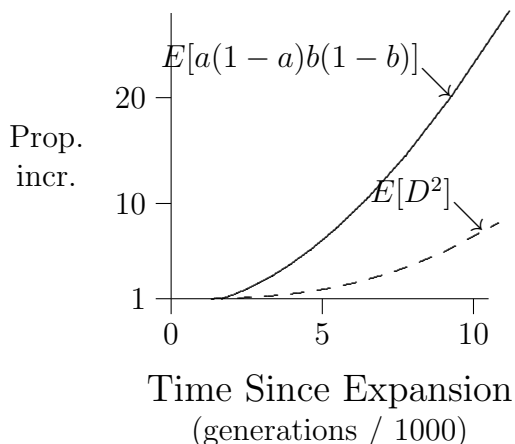
## Effect of a bottleneck

Figure 7 shows the effect of a 100-generation bottleneck in population size. Before and after the bottleneck, this population had size  $2N = 10^5$ . During the bottleneck, its size was  $10^3$ . The bottleneck ended at time 0, and we observe it in various subsequent generations. In the graph, the curve labeled  $t = 0$  is at the end of the bottleneck and exhibits an LD curve that is high but flat, for reasons discussed in the preceding paragraph. As time passes, the right portion of the curve (the portion with high rates of recombination) falls much faster than the left, so that by generation 1000, the curve is almost L-shaped. This is the signature of a bottleneck in population size.

Why should there be such a difference between expansion from an initial equilibrium and from a bottleneck?—between Figs. 2 and 7? Both curves are declining toward the same equilibrium, but the left portion of the curve declines much more slowly after a bottleneck than after expansion from equilibrium. This can only reflect the state of the initial population, just before the increase in size. The initial population of Fig. 2 had been small much longer than that of Fig. 7. Consequently, it had less heterozygosity. As we shall see in the next section, this accelerates the rate of decline.



**Figure 8: The time path of  $\sigma_d^2$  after a population expansion.** The initial population was small ( $2N = 10^3$ ) and at mutation-drift equilibrium. At time 0 it expands suddenly to a much larger size ( $2N = 10^5$ ). Each curve shows the time path of  $\sigma_d^2$  for a different rate of recombination, measured in centimorgans (cM). There is a curve for tight linkage ( $\bullet$ , 0.02 cM), one for somewhat weaker linkage ( $\star$ , 0.3 cM), and one for linkage that it weaker still ( $\circ$ , 1 cM). Dotted lines connect the final value of each curve to its ultimate equilibrium, which would be reached if the population stayed large forever.



**Figure 9: The time path of numerator and denominator of  $\sigma_d^2$  following a population expansion.** Dashed line shows numerator of  $\sigma_d^2$ , relative to its value in generation 1000. Solid line shows the denominator in the same way. Loci are separated by 0.02 cM. Population history is as in Fig. 8.

### The time paths of individual points on the LD curve

Figure 8 shows the time path of  $\sigma_d^2$  after an expansion in population size. Because the new population is larger, the new equilibrium will have less LD. But  $\sigma_d^2$  does not decline monotonically toward this new equilibrium. Instead, it falls rapidly to a smaller value before climbing back slowly towards to the new equilibrium.

The initial decline in  $\sigma_d^2$  does not result from any decline in its numerator,  $E[D^2]$ . Indeed, Fig. 9 shows that the numerator actually grows. The decline in

$\sigma_d^2$  happens because growth in its numerator is outstripped by that in its denominator,  $E[a(1-a)b(1-b)]$ , which increases under the influence of mutation. The proportional increase is large, because our initial population that was small and therefore had little heterozygosity. For this reason, the denominator was initially so small that increments caused by mutation had a large proportional effect.

Two factors account for the post-expansion growth in  $E[D^2]$ , the numerator of  $\sigma_d^2$ . First,  $D$  is proportional to heterozygosity (KAPLAN and WEIR, 1992, p. 334), which increases in response to mutation. Ordinarily, the positive effect on  $D^2$  would be offset by the negative effect of recombination. But in the early generations following our expansion, this negative effect is very weak. This is because the initial population was small and thus had low heterozygosity. Few recombinant gametes are produced in such a population, because such gametes are produced only by double heterozygotes. Consequently, the effect of recombination is weaker than that of mutation.

The non-monotone time path in Fig. 8 refers to  $\sigma_d^2$ , but it seems plausible that  $r^2$  might obey similar dynamics. This may explain why, in the right panel of Fig. 2, the left end of the curve for  $t = 500$  is below the equilibrium.

This also explains why the left portion of the LD curve declines faster after

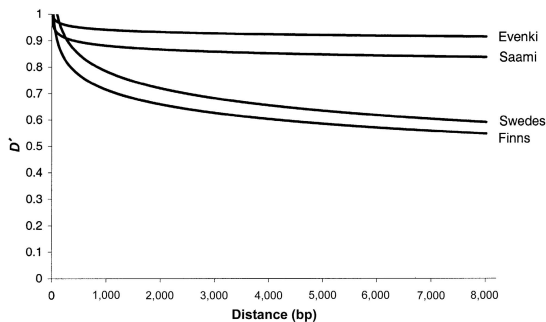


**Figure 10: LD curves for four human populations.** Source: KAESSMANN *et al.* (2002, Fig. 3).

expansion from equilibrium than after a bottleneck. The left portion of the curve refers to tightly-linked sites, with weak recombination. In the post-expansion population, genetic drift is also weak because the population is large. Because recombination and drift are both weak, mutation dominates the dynamics. The proportional effect of mutation is large when heterozygosity is low. In the case of expansion from equilibrium, the population has been small a long time, so heterozygosity is low, the proportional effect of mutation is large, and  $\sigma_d^2$  declines rapidly. Heterozygosity is not so low at the end of a bottleneck, because the population has been small only briefly. Consequently, the proportional effect of mutation is smaller, and  $\sigma_d^2$  declines more slowly.

## LD in real populations

When applied to data from real populations, the present methods may suggest one history or another. Such suggestions can only be tentative, because they take no account of statistical uncertainty. Nonetheless, they may be useful in exploratory data analysis. In this spirit, let us examine the LD curves of several human populations.

Figure 10 shows LD curves published by KAESSMANN *et al.* (2002) for four populations. They measure LD using the statistic  $D'$ , which is a normalized variant of  $D$  (LEWONTIN, 1964, p. 55). Two of the curves—those for the Evenki and the Saami—refer to small high-latitude foraging populations. The other two refer to the large populations of nation states. The curves of the two foraging populations are not only high, but also much flatter than those of the nation states. They resemble the dashed lines in Fig. 6. KAESSMANN *et al.* (2002, p. 681) attribute elevated LD in the foraging populations to a long history of constant size. The present analysis, however, suggests a different interpretation. If  $D'$  behaves like  $\hat{\sigma}_d^2$ , the flat LD curves suggest that both foraging populations have recently declined in size. On the basis of similar data, PRITCHARD and PRZEWORSKI (2001, p. 7) suggest a third hypothesis—recent admixture—which is also plausible.

In Fig. 11, the open circles show  $\hat{\sigma}_d^2$  values estimated from chromosome 1 in

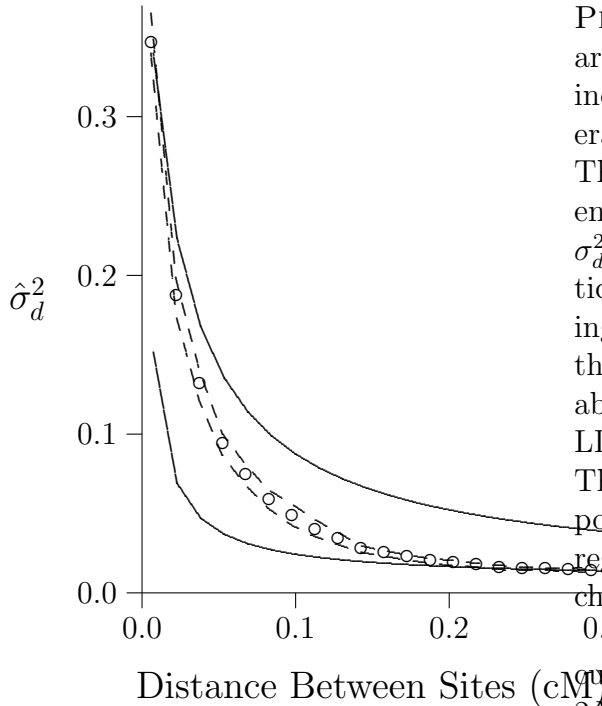


**Figure 11: LD curve for chromosome 1 in Europe.** Open circles show the estimated values of  $\sigma_d^2$ , and dashed lines show a 95% bootstrap confidence region, generated by moving-blocks bootstrap. Solid lines show the equilibrium curves for  $2N = 5000$  and  $2N = 30,000$ . All analyses are based on a sample of 120 chromosomes. Source: CEU data set from the 1000-Genomes project (THE 1000 GENOMES PROJECT CONSORTIUM, 2012). Genetic map data, downloaded from the 1000-Genomes website, were estimated from phased haplotypes in HapMap Release 22 (NCBI 36) (HAPMAP, 2007).

European data (THE 1000 GENOMES PROJECT CONSORTIUM, 2012). These are surrounded by dashed lines, which indicate a 95% confidence region generated by moving blocks bootstrap. These show that chromosome 1 provides enough data for accurate estimates of  $\sigma_d^2$ . In 1981, HILL (1981) expressed skepticism about the possibility of estimating population size from data on LD. At that time only limited data were available, and it was not possible to estimate LD statistics with any great accuracy. This inaccuracy bled into estimates of population size. The narrow confidence region in Fig. 11 shows that things have changed.

The solid lines show equilibrium curves for the cases  $2N = 5000$  and  $2N = 30,000$ . Clearly, the observed curve declines more steeply than either equilibrium curve. As we have seen, this suggests a history of population expansion in Europe, in agreement with many other analyses of European data. To go farther than this, we would need to fit parameters describing population history. Methods for this purpose will be described in a separate publication.

## DISCUSSION

$\sigma_d^2$  has never been valued for its own sake. It is seen instead as an approximation to the quantity of real interest—the expected value of  $r^2$ . Yet it is often a poor approximation, even in pop-

ulations of constant size (MARUYAMA, 1982; HUDSON, 1985, pp. 616–617). It is even worse when population size varies.

Following a change in population size, the mean of  $r^2$  converges toward its new equilibrium far faster than does  $\sigma_d^2$ . Presumably, this is because  $\sigma_d^2$  is sensitive to loci with high heterozygosity, and the gene trees of such loci are deep. Whatever the cause, this difference in rates of convergence has two effects. First, it makes  $\sigma_d^2$  useless as an approximation to  $r^2$  in populations that have varied in size. On the other hand, it also means that  $\sigma_d^2$  itself provides a deep record of demographic history.

To take advantage of this extended record, one must estimate  $\sigma_d^2$  directly from data. This is easy to do, by using averages in place of the expectations in Eqn. 2. With genome-scale data, such estimates are quite accurate. This provides a measure of LD that is unique in that one can easily calculate expected LD from the history of population size. With other measures, such inferences would require extensive computer simulations.

Following a population expansion, drift is weak and the dynamics of LD are dominated by recombination. The LD curve begins to decline, and this decline is fastest in the right-hand portion of the curve, where recombination rates are highest. Consequently, the curve will be unusually steep for hundreds of generations following a population expansion.

tion.

Following a population collapse, drift becomes strong and dominates the dynamics. It pushes LD upward rapidly and relatively uniformly throughout the curve. Thus, the LD curve becomes high and flat. This may explain a phenomenon that puzzled PRITCHARD and PRZEWORSKI (2001, p. 7):

We have several examples in which large regions exhibit more LD than would be expected under either a model of constant population size or a mode with rapid population growth. Yet, at the same time studies of polymorphism at a small scale reveal less LD than would be expected. These observations at different scales are hard to accommodate in a single explanation since factors that increase long-distance LD will tend to have an even larger effect on closely linked sites.

As we have seen, this pattern arises naturally from a recent reduction in population size.

A bottleneck in population size begins with an episode of population collapse. At the end of the bottleneck, the LD curve is therefore high but flat. As population size rises at the end of the bottleneck, genetic drift becomes weak and recombination grows in importance. The right portion of the LD curve falls

faster than the left, so the curve becomes steeper.

In the left portion of the curve, recombination is weak. Genetic drift is also weak, because of the increase in population size. This allows mutation to play an important role, and its effect distinguishes the two forms of expansion: from equilibrium and from a bottleneck. In the former case, the pre-expansion population had little heterozygosity, so each mutational increment has a large proportional effect on the denominator of  $\sigma_d^2$ . After a bottleneck, the opposite is true, so the left portion of the LD curve declines more slowly. The curve becomes even steeper after a bottleneck than after an expansion from equilibrium.

In summary, (1) when recombination is strong relative to drift, LD declines and the curve becomes steeper; (2) when drift is strong relative to recombination, LD rises but the curve stays flat; and (3) where drift and recombination are both weak, the rate of decline in LD decreases with heterozygosity.

The LD curves of two foraging populations are high and flat, suggesting a recent collapse of population size. The European population, on the other hand, has a curve that is quite steep, suggesting a history of population expansion. This might reflect the spread of modern humans into Europe, the spread of farmers during the Neolithic, or the spread of Indo-European speakers.

## ACKNOWLEDGEMENTS

I am grateful for comments from R. Bohlender, E. Cashdan, R. Gutenkunst, H. Harpending, W.G. Hill, and J. Seger and for access to computer facilities in the laboratories of Lynn Jorde and Henry Harpending.

## APPENDIX

### Hill's model of LD evolution

HILL (1975) incorporates mutation using the model of infinite alleles. However, most modern work involves either DNA sequence data, or single nucleotide polymorphisms (SNPs). In these data, alleles are nucleotide states: A, T, G, or C. Nearly all loci have just two alleles, so it is not appropriate to assume an infinity of alleles. Yet as we shall see, Hill's (1975) results also apply to a more appropriate mutational model—that of “infinite sites” (KIMURA, 1969), which assumes that mutation never strikes the same site twice.

Hill begins with a vector of moments, associated with alleles  $A_h$ ,  $A_i$ ,  $B_j$ , and  $B_k$  at loci  $A$  and  $B$ :

$$y_{hi,jk} = \begin{pmatrix} E[a_h a_i b_j b_k] \\ E[a_h b_j D_{ik} + a_h b_k D_{ij} \\ + a_i b_j D_{hk} + a_i b_k D_{hj}] \\ E[D_{hj} D_{ik} + D_{hk} D_{ij}] \end{pmatrix}$$

Here  $a_i$  and  $b_j$  are the frequencies of allele  $A_i$  at locus  $A$  and allele  $B_j$  at lo-

cus  $B$ . The disequilibrium coefficients,  $D_{ij}$ , are defined such that  $a_i b_j + D_{ij}$  is the frequency of gamete type  $A_i B_j$ . The dynamics of these moments are approximately linear, after dropping terms in  $u^2$ ,  $1/N^2$ , and  $u/N$ , where  $u$  is the mutation rate and  $N$  the diploid population size. Thus, HILL (1975, Eqn. 1) shows that

$$y_{hi,jk}(t+1) \approx \mathbf{DRM}y_{hi,jk}(t)$$

where  $\mathbf{D}$ ,  $\mathbf{R}$ , and  $\mathbf{M}$  are matrices describing the linear effects of drift, recombination, and mutation. So far, the model describes only the changes in frequency of existing alleles. Thus it applies not only to Hill's model of infinite alleles, but also to the model of infinite sites.

To incorporate mutation, Hill defines a new vector,

$$x = \sum_{h \neq i} \sum_{j \neq k} y_{hi,jk} \quad (5)$$

where the sums run across all pairs of alleles at each locus. The dynamics of this new vector include an additive contribution,  $\Delta x_{\text{mut}}$ , which represents the effect of mutation to new alleles:

$$x(t+1) \approx \mathbf{DRM}x(t) + \Delta x_{\text{mut}}(t) \quad (6)$$

This equation can be iterated across many generations, and it is easy to incorporate changes in population size. At the end of this process,  $\sigma_d^2$  is calculated as  $x_3/2x_1$  (HILL, 1975, p. 124).

The first term on the right side of Eqn. 6 applies equally to both mutational models. Some reinterpretation is required, however, to relate the second term to the model of infinite sites. In this new context,  $\Delta x_{\text{mut}}$  becomes the contribution of mutations at other sites in the genome, rather than that from new alleles at the same pair of sites. The mutational increments are however identical in the two models, as we shall see.

To see that this is so, let us take a close look at the mutational contributions to  $x$ , the vector defined above in Eqn. 5. Under the model of infinite sites, mutation never strikes the same site twice, so each polymorphic site has exactly two alleles. In this biallelic context, we can simplify Hill's vector of moments as

$$h = \begin{pmatrix} E[a(1-a)b(1-b)] \\ E[(1-2a)(1-2b)D] \\ E[D^2] \end{pmatrix} \quad (7)$$

Here,  $a$  and  $b$  are the frequencies of alleles  $A_1$  and  $B_1$ , and  $D$  is the coefficient of linkage disequilibrium. It is defined such that the  $ab + D$  is the frequency of gamete type  $A_1 B_1$ . When each locus is biallelic, Hill's multiallelic moments reduce to  $x_1 = 4h_1$ ,  $x_2 = 4h_2$ , and  $x_3 = 8h_3$  (HILL, 1975, p. 123).

The mutational increments,  $\Delta x_{\text{mut}}$  and  $\Delta h_{\text{mut}}$ , both depend on the heterozygosity,  $H = E[2a(1-a)]$ . The dynamics of heterozygosity under infinite

sites are the same as those under infinite alleles (HILL, 1975, p. 120):

$$H_{t+1} \approx 2u + (1 - 1/2N - 2u)H_t$$

The  $h_i$  are nonzero only if both loci are polymorphic. On the other hand, our model assumes that mutation affects only monomorphic sites. This implies that mutational increments to  $h$  occur only at pairs of sites in which one site is polymorphic and the other monomorphic. Table 1 summarizes the case in which  $A$  is initially polymorphic, and a mutation strikes an initially monomorphic locus,  $B$ .

Consider first the increment to  $h_1 = E[a(1 - a)b(1 - b)]$ . Before mutation,  $h_1 = 0$  because  $b = 0$ . After mutation,  $b = 1/2N$ , so  $h_1$  becomes  $E[a(1 - a)(1/2N - 1/4N^2)] \approx H/4N$ . This accounts for only half the effect of mutation, because there are also pairs at which  $A$  is monomorphic and  $B$  polymorphic. The expected effect of a single mutation is thus approximately  $H/2N$ . The expected number of such mutations per generation is  $2Nu$ . In aggregate, therefore, the increment from mutation is  $\Delta_{\text{mut}}h_1 \approx uH$ .

To derive the mutational increment to  $h_2 = E[(1 - 2a)(1 - 2b)D]$ , we assume as before that  $A$  is polymorphic but  $B$  is not. Because  $D$  is zero when either site is monomorphic,  $h_2 = 0$  before mutation. After mutation, there are two cases to consider. With probability  $a$ , the mutation falls on an  $A_1$ -

bearing gamete, and  $h_2$  becomes  $(1 - 2a)(1 - 2/2N)(1 - a)/2N$ , as shown in Table 1. On the other hand, with probability  $1 - a$  the mutation falls on an  $A_0$ -bearing gamete, and  $h_2$  becomes  $-(1 - 2a)(1 - 2/2N)a/2N$ . In expectation, the new value of  $h_2$  is 0. This result is conditional on a mutation at locus  $B$ , but an identical argument applies for mutation at locus  $A$ . Thus,  $\Delta_{\text{mut}}h_2 = 0$ .

The third moment is  $h_3 = E[D^2]$ . Because  $B$  is initially monomorphic,  $D^2 = 0$  before the mutation. When a mutation occurs at  $B$ , it strikes an  $A_1$ -bearing gamete with probability  $a$  and an  $A_0$ -bearing gamete with probability  $1 - a$ . The resulting values of  $D$  are shown in table 1. Squaring these and weighting by  $a$  and  $1 - a$  gives

$$\begin{aligned} E[a\{(1 - a)^2/4N^2\} + (1 - a)\{a^2/4N^2\}] \\ = H/8N^2, \end{aligned}$$

This is the effect on  $D^2$  of a single mutation at  $B$ . There are  $2Nu$  such mutations per generation, so the expected increment from mutation at locus  $B$  is  $2Nu \times H/8N^2 = uH/4N$ . Finally, multiply by 2 to account for cases in which  $A$  is initially monomorphic and  $B$  polymorphic. This gives  $\Delta_{\text{mut}}h_3 = uH/2N \approx 0$ , ignoring terms of order  $u/N$ .

In summary,

$$\Delta_{\text{mut}}h \approx [uH, 0, 0], \quad (8)$$

in agreement with HILL (1975, p. 121). This shows that the mutational incre-

**Table 1:** Effect of a single mutation at  $B$ , assuming that  $A$  is initially polymorphic.

	Gamete frequencies				$D$
	$A_1B_1$	$A_1B_0$	$A_0B_1$	$A_0B_0$	
General	$w$	$x$	$y$	$z$	$wz - xy$
Before mutation	0	$a$	0	$1 - a$	0
$A_1$ -linked mutation	$1/2N$	$a - 1/2N$	0	$1 - a$	$(1 - a)/2N$
$A_2$ -linked mutation	0	$a$	$1/2N$	$1 - a - 1/2N$	$-a/2N$

ment is the same under the models of infinite sites and infinite alleles. Because of this equivalence, Hill's results apply equally to both models of mutation.

### Estimating Linkage Disequilibrium with Partially Phased Diploid Data

In 1000-genotypes data, many genotypes are phased but not all. At different loci, the unphased genotypes may correspond to different individuals. Thus, we need a method that can deal unphased genotypes that are scattered throughout the data matrix.

The symbols  $j$ ,  $k$ ,  $l$ , and  $m$  represent alleles and will always equal either 0 or 1. I will write phased two-locus genotypes in form  $\begin{smallmatrix} jk \\ lm \end{smallmatrix}$ , which says that a diploid individual has genotype  $jk$  at locus  $A$ , and genotype  $lm$  at locus  $B$ . This represents the union of gametes  $\begin{smallmatrix} j \\ l \end{smallmatrix}$  and  $\begin{smallmatrix} k \\ m \end{smallmatrix}$ . This genotype is unordered, in that we cannot distinguish the maternal gamete from the paternal one. Consequently, there is no distinction between

$\begin{smallmatrix} jk \\ lm \end{smallmatrix}$  and  $\begin{smallmatrix} kj \\ ml \end{smallmatrix}$ . When I write genotypes in this form, I imply that linkage phase is known. In other words, genotypes  $\begin{smallmatrix} jk \\ lm \end{smallmatrix}$  and  $\begin{smallmatrix} kj \\ ml \end{smallmatrix}$  are not equivalent.

Consider a tiny two-locus data set, consisting of three diploid individuals.

$$G_1, G_1, G_3 = \begin{matrix} j_1k_1 & j_2k_2 & j_3k_3 \\ l_1m_1 & l_2m_2 & l_3m_3 \end{matrix}$$

On the right, each row corresponds to a locus, and each column to a gamete. To estimate linkage disequilibrium ( $D$ ), we would need to calculate  $S = \sum_{i=1}^6 x_i y_i$ , where  $x_i$  is the  $i$ th value in the upper row and  $y_i$  is the corresponding value in the lower one. This sum can be written as

$$\begin{aligned} S &= s_1 + s_2 + s_3 \\ &= (j_1l_1 + k_1m_1) + (j_2l_2 + k_2m_2) \\ &\quad + (j_3l_3 + k_3m_3) \end{aligned}$$

Here,  $s_i = j_i l_i + k_i m_i$  is the contribution of the  $i$ th diploid genotype. This calculation requires phased data, and it is the only step where such data are required in estimating  $D$ . To cope with unphased data, we need a method to estimate  $s_i$ .

Consider the function  $s \binom{jk}{lm} = jl + km$ . If at least one genotype is homozygous then phasing doesn't matter. For example,  $s \binom{jk}{u} = s \binom{kj}{u}$ . We can calculate  $s$  regardless of phasing. The only genotypes that need concern us are those in which both loci are heterozygous.

As mentioned above, all genic values ( $j, k, l$ , and  $m$ ) are either 0 or 1. Double heterozygotes will look either like  $\begin{smallmatrix} 01 \\ 01 \end{smallmatrix}$  or  $\begin{smallmatrix} 01 \\ 10 \end{smallmatrix}$ . (I ignore the equivalent representations  $\begin{smallmatrix} 10 \\ 10 \end{smallmatrix}$  and  $\begin{smallmatrix} 10 \\ 01 \end{smallmatrix}$ , because genotypes are unordered.) With unphased data, we cannot distinguish between these two genotypes. Yet they imply different values:  $s \binom{01}{01} = 1$  but  $s \binom{01}{10} = 0$ . For double heterozygotes, I replace  $s$  with its expected value, which equals the probability,  $w$ , that the genotype is of form  $\begin{smallmatrix} 01 \\ 01 \end{smallmatrix}$  rather than  $\begin{smallmatrix} 01 \\ 10 \end{smallmatrix}$ .

To calculate this probability, I begin with standard results for the frequencies of the four gamete types, as shown in Table 2. Following ROGERS and HUFF (2009), I ignore recombination in the most recent generation. Under random mating, these gametes form at random to produce two-locus genotypes. The frequency of genotype  $\begin{smallmatrix} 01 \\ 01 \end{smallmatrix}$  among double heterozygotes is thus

$$\begin{aligned} w &= \frac{2p_0p_3}{2p_0p_3 + 2p_1p_2} \\ &= \frac{D + Z}{D + 2Z} \end{aligned} \quad (9)$$

**Table 2:** Gamete types and frequencies.  $n_i$  is the number of copies of gamete  $i$  in the sample, excluding unphased double heterozygotes.  $p_i$  is the frequency of that gamete type within the population.  $a$  is the frequency of allele 1 at locus  $A$ ,  $b$  the frequency of 1 at  $B$ , and  $D$  the conventional coefficient of linkage disequilibrium.

Gamete	Sample count	Population frequency
$\begin{smallmatrix} 0 \\ 0 \end{smallmatrix}$	$n_0$	$p_0 = (1 - a)(1 - b) + D$
$\begin{smallmatrix} 0 \\ 1 \end{smallmatrix}$	$n_1$	$p_1 = (1 - a)b - D$
$\begin{smallmatrix} 1 \\ 0 \end{smallmatrix}$	$n_2$	$p_2 = a(1 - b) - D$
$\begin{smallmatrix} 1 \\ 1 \end{smallmatrix}$	$n_3$	$p_3 = ab + D$

where

$$\begin{aligned} Z &= \alpha - \beta D + D^2, \\ \alpha &= a(1 - a)b(1 - b), \quad \text{and} \\ \beta &= a + b - 2ab. \end{aligned}$$

These results can be used to estimate  $D$  using the EM algorithm (DEMPSTER *et al.*, 1977). Let  $K$  represent the number of unphased double heterozygotes. Each of these is of type  $\begin{smallmatrix} 01 \\ 01 \end{smallmatrix}$  with probability  $w$  and of type  $\begin{smallmatrix} 01 \\ 10 \end{smallmatrix}$  with probability  $1 - w$ . The expected log likelihood is

$$\begin{aligned} E \ln L &= \sum_{i=0}^3 n_i \ln p_i + K[w(\ln p_0 + \ln p_3) \\ &\quad + (1 - w)(\ln p_1 + \ln p_2)] \\ &= (n_0 + Kw) \ln p_0 \end{aligned}$$

$$\begin{aligned}
&+ (n_1 + K(1 - w)) \ln p_1 \\
&+ (n_2 + K(1 - w)) \ln p_2 \\
&+ (n_3 + Kw) \ln p_3
\end{aligned}$$

Note that  $E \ln L$  depends on  $p_0, p_1, p_2,$  and  $p_3$ , which are themselves functions of  $D$ . The maximum-likelihood estimate of  $D$  is the value that maximizes  $E \ln L$ .

This is a unidimensional maximization problem, because  $D$  is the only unknown.  $D$  cannot fall outside the range  $[\underline{D}, \overline{D}]$ , where  $\underline{D}$  is the maximum of  $-a(1-b)$  and  $-b(1-a)$ , and  $\overline{D}$  the minimum of  $a(1-b)$  and  $b(1-a)$  (LEWONTIN, 1964, p. 55). The initial value of  $D$  is set assuming that  $w = 1/2$ . In each iteration, if  $d^2 E \ln L / dD^2 < 0$ , then the algorithm tries a Newton step (HAMMING, 1973, p. 68). If the result is within  $[\underline{D}, \overline{D}]$ , then the Newton step is accepted. Otherwise, the algorithm uses a modified version of the bisection algorithm (HAMMING, 1973, p. 62) to move in the uphill direction, as indicated by the sign of  $dE \ln L / dD$ .

The modification to bisection allows the algorithm to make large steps when it seems likely that the optimum is at a boundary. For example, if  $dE \ln L / dD > 0$  at the current value of  $D$ , then motion is to the right, toward  $\overline{D}$ . Before deciding how far to move, the algorithm checks the sign of the derivative at  $\overline{D}$ . If both derivatives are positive, then the algorithm takes a big step, moving 80% of the distance from  $D$  to  $\overline{D}$ . But if the two derivatives have op-

posite sign, then the algorithm takes a small step, moving only 50% of the way to  $\overline{D}$ . When  $dE \ln L / dD < 0$ , the algorithm is similar, except that motion is to the left, toward  $\underline{D}$ .

## REFERENCES

- CHEN, G. K., P. MARJORAM, and J. D. WALL, 2009 Fast and flexible simulation of DNA sequence data. *Genome Research* **19**: 136–142.
- CLARK, A. G., M. J. HUBISZ, C. D. BUSTAMANTE, S. H. WILLIAMSON, and R. NIELSEN, 2005 Ascertainment bias in studies of human genome-wide polymorphism. *Genome Research* **15**: 1496–1502.
- DEMPSTER, A. P., N. M. LAIRD, and D. B. RUBIN, 1977 Maximum likelihood from incomplete data via the EM algorithm. *Journal of the Royal Statistical Society, Series B* **39**: 1–38.
- DURRETT, R., 2008 *Probability Models for DNA Sequence Evolution*. Springer, New York, second edition.
- FRISSE, L., R. HUDSON, A. BARTOSZEWICZ, J. WALL, J. DONFACK, and A. DI RIENZO, 2001 Gene conversion and different population histories may explain the contrast between polymorphism and linkage disequilibrium levels. *American Journal of Human Genetics* **69**: 831–843.

- FU, Y., 1995 Statistical properties of segregating sites. *Theoretical Population Biology* **48**: 172–197.
- GRIFFITHS, R. and S. TAVARÉ, 1998 The age of a mutation in a general coalescent tree. *Stochastic Models* **14**: 273–295.
- HAMMING, R. W., 1973 *Numerical Methods for Scientists and Engineers*. Dover Publications, second edition.
- HAPMAP, 2007 A second generation human haplotype map of over 3.1 million SNPs. *Nature* **449**: 851–862.
- HAYES, B., P. VISSCHER, H. MCPARTLAN, and M. GODDARD, 2003 Novel multilocus measure of linkage disequilibrium to estimate past effective population size. *Genome Research* **13**: 635.
- HILL, W. G., 1975 Linkage disequilibrium among multiple neutral alleles produced by mutation in finite population. *Theoretical Population Biology* **8**: 117–126.
- HILL, W. G., 1981 Estimation of effective population size from data on linkage disequilibrium. *Genetical Research, Cambridge* **38**: 209–216.
- HILL, W. G. and A. ROBERTSON, 1968 Linkage disequilibrium in finite populations. *Theoretical and Applied Genetics* **38**: 226–231.
- HUDSON, R. R., 1985 The sampling distribution of linkage disequilibrium under an infinite allele model without selection. *Genetics* **109**: 611–631.
- KAESSMANN, H., S. ZÖLLNER, A. C. GUSTAFSSON, V. WIEBE, M. LAAN, J. LUNDEBERG, M. UHLÉN, and S. PÄÄBO, 2002 Extensive linkage disequilibrium in small human populations in eurasia. *The American Journal of Human Genetics* **70**: 673–685.
- KAPLAN, N. and B. WEIR, 1992 Expected behavior of conditional linkage disequilibrium. *American Journal of Human Genetics* **51**: 333.
- KIMURA, M., 1969 The number of heterozygous nucleotide sites maintained in a finite population due to steady flux of mutation. *Genetics* **61**: 893–903.
- KRUGLYAK, L., 1999 Prospects for whole-genome linkage disequilibrium mapping of common disease genes. *Nature Genetics* **22**: 139–144.
- LEWONTIN, R. C., 1964 The interaction of selection and linkage. I. General considerations; heterotic models. *Genetics* **49**: 49–67.
- LEWONTIN, R. C., 1967 An estimate of average heterozygosity in man. *American Journal of Human Genetics* **19**: 681–685.

- LIEU, R. Y. and K. SINGH, 1992 Moving blocks jackknife and bootstrap capture weak dependence. In *Exploring the "Limits" of the Bootstrap*, edited by R. LePage and L. Billard, pp. 225–248, Wiley, New York.
- LITTLER, R., 1973 Linkage disequilibrium in two-locus, finite, random mating models without selection or mutation. *Theoretical Population Biology* **4**: 259–275.
- MARUYAMA, T., 1982 Stochastic integrals and their application to population genetics. In *Molecular Evolution, Protein Polymorphism, and the Neutral Theory*, edited by M. Kimura, pp. 151–166, Springer-Verlag, Berlin.
- MCEVOY, B., J. POWELL, M. GODDARD, and P. VISSCHER, 2011 Human population dispersal “out of Africa” estimated from linkage disequilibrium and allele frequencies of SNPs. *Genome Research* **21**: 821–829.
- MCVEAN, G., 2002 A genealogical interpretation of linkage disequilibrium. *Genetics* **162**: 987–991.
- OHTA, T. and M. KIMURA, 1969 Linkage disequilibrium at steady state determined by random genetic drift and recurrent mutation. *Genetics* **63**: 229.
- OHTA, T. and M. KIMURA, 1971 Linkage disequilibrium between two segregating nucleotide sites under the steady flux of mutations in a finite population. *Genetics* **68**: 571–580.
- PRITCHARD, J. and M. PRZEWORSKI, 2001 Linkage disequilibrium in humans: Models and data. *American Journal of Human Genetics* **69**: 1–14.
- ROGERS, A. R. and C. HUFF, 2009 Linkage disequilibrium between loci of unknown phase. *Genetics* **182**: 839–844.
- ROGERS, A. R. and L. B. JORDE, 1996 Ascertainment bias in estimates of average heterozygosity. *American Journal of Human Genetics* **58**: 1033–1041.
- SCHAPER, E., A. ERIKSSON, M. RAFAJLOVIC, S. SAGITOV, and B. MEHLIG, 2012 Linkage disequilibrium under recurrent bottlenecks. *Genetics* **190**: 217–229.
- SONG, Y. and J. SONG, 2007 Analytic computation of the expectation of the linkage disequilibrium coefficient  $r^2$ . *Theoretical Population Biology* **71**: 49–60.
- STROBECK, C. and K. MORGAN, 1978 The effect of intragenic recombination on the number of alleles in a finite population. *Genetics* **88**: 829–844.
- SVED, J. A., 1971 Linkage disequilibrium and homozygosity of chromosome segments in finite popula-

- tions. *Theoretical Population Biology* **2**: 125–141.
- SVED, J. A., 2009 Correlation measures for linkage disequilibrium within and between populations. *Genetical Research, Cambridge* **91**: 183–192.
- SVED, J. A. and M. W. FELDMAN, 1973 Correlation and probability methods for one and two loci. *Theoretical Population Biology* **4**: 129–132.
- TENESA, A., P. NAVARRO, B. HAYES, D. DUFFY, G. CLARKE, M. GODDARD, and P. VISSCHER, 2007 Recent human effective population size estimated from linkage disequilibrium. *Genome Research* **17**: 520–526.
- THE 1000 GENOMES PROJECT CONSORTIUM, 2012 An integrated map of genetic variation from 1,092 human genomes. *Nature* **491**: 56–65.
- WEIR, B. and C. COCKERHAM, 1974 Behavior of pairs of loci in finite monoecious populations. *Theoretical Population Biology* **6**: 323–354.
- WEIR, B. S., 1996 *Genetic Data Analysis II: Methods for Discrete Population Genetic Data*. Sinauer, Sunderland, MA.